

Synthesis, Characterization and Property Studies on a Dinuclear Copper(II) Complex with Dipyridine Derivate and Acetylacetonone

Pu Su Zhao,* Zhi Yan Guo, Jing Sui, Jing Wang, and Fang Fang Jian

New Materials & Function Coordination Chemistry Laboratory, Qingdao University of Science and Technology, Qingdao Shandong 266042, P. R. China. *E-mail: zhaopusu@163.com
Received August 10, 2010, Accepted September 30, 2010

A dinuclear copper(II) complex of $[\text{Cu}_2(\text{aceace})_4(\text{dipyph})]$ [aceace = acetylacetonone, dipyph = 1,4-di(4-pyridyl-ethene-2-yl)-benzene] has been synthesized and characterized by elemental analysis, IR and X-ray single crystal diffraction. It crystallizes in the monoclinic system, space group $P2_1/c$, with lattice parameters $a = 7.9584(16) \text{ \AA}$, $b = 18.594(4) \text{ \AA}$, $c = 15.063(4) \text{ \AA}$, $\beta = 120.97(2)^\circ$ and $M_r = 807.85$ ($\text{C}_{40}\text{H}_{44}\text{Cu}_2\text{N}_2\text{O}_8$), $Z = 2$. Each of the Cu^{2+} ion adopts a square pyramid geometry and coordinates with four oxygen atoms from two aceace ligands and one nitrogen atom from dipyph bidentate ligand. Magnetic measurement shows that the Weiss constant and Curie constant for the title compound are -0.22 K and $0.1154 \text{ emu}\cdot\text{K}/\text{mol}$, respectively. Thermal stability data indicate that the title complex undergoes two steps decomposition and the residue is Cu_2O_4 . In the potential range of $-1.5 \sim 0.8 \text{ V}$, the title complex represents an irreversible electrochemical process.

Key Words: Dinuclear Cu complex, Crystal structure, Magnetic property, Thermal stability, Electrochemical property

Introduction

Construction of supramolecular architectures with interesting physical properties has grown rapidly owing to their potentiality as new functional material.¹⁻⁴ The most efficient and widely used approach for designing such material is the self-assembly of organic ligands and metal ions, and the type/topology of the products generated from this process can be tuned by a judicious choice of the ligands,⁵⁻⁶ metal coordination geometry preference, counter ion,⁶⁻⁸ solvent,⁸⁻⁹ metal to ligand ratio¹⁰⁻¹¹ and temperature.¹² Among these, the choice of organic ligand is one of the important factors. Organic chelating ligands block some coordination sites whereas organic spacers serve to link metal sites and to propagate the structural information expressed in the metal coordination preferences through the extended structure. The properties of the organic spacers, such as solubility, coordination activity, length, geometry and relative orientation of the donor groups play a very important role in dictating polymer framework topology and even in affecting the formation of polymer vs. oligomer vs. molecule.

Most commonly used organic spacers for designing the coordination architecture are pyrazine,¹³⁻¹⁴ bridged bidentate bipyridyl ligands¹⁵⁻¹⁷ and nitrile substituted pyridine.¹⁸ For designing dinuclear metal complex, an unsaturated coordination environment for single coordinated metal and the presence of a bridging atom or ligands are essential. In addition, the reaction conditions appear crucial in designing the dinuclear complexes.¹⁹ Herein, we report the synthesis, crystal structure and properties of a dinuclear copper(II) complex with a bridged bidentate bipyridyl ligand of 1,4-di(4-pyridylethene-2-yl)-benzene(dipyph), which was synthesized by our group, and the organic chelating ligand of acetylacetonone (aceace).

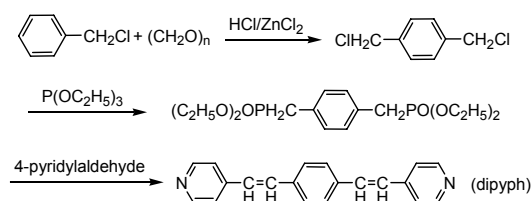
Experimental Section

All reagents were purchased from commercial sources and

used without further purification. Element analyses were performed on a Perkin-Elmer 2400LS elemental analyzer. The melting points were determined on a Yanaco MP-500 melting point apparatus. IR spectra were recorded from 4000 to 400 cm^{-1} using KBr pellets on a Nicolet AVATAR360 instrument. ¹H NMR spectra were recorded in DMSO at room temperature at 400 MHz on a Bruker instrument. The magnetic susceptibilities were performed on a Quantum Design MPMS-7 SQUID magnetometer. Thermogravimetry (TG) and differential thermal gravimetric (DTG) analysis were carried out on a SDR 2980 simultaneously for the samples of 10 mg at a heating rate of 10 $^\circ\text{C}/\text{min}$.

Preparation of $[\text{Cu}_2(\text{aceace})_4(\text{dipyph})]$. Firstly, according to the methods reported earlier,²⁰⁻²² the bridged bidentate bipyridyl ligand of 1,4-di(4-pyridylethene-2-yl)-benzene(dipyph) was synthesized and synthetic path is showed in Scheme 1. The products of dipyph were yellow powders. Yield 95.1%. mp 282.4 - 284.1 $^\circ\text{C}$. Anal. Calcd (%): C, 84.47; H, 5.67; N, 9.85; Found (%): C, 84.31; H, 5.54; N, 9.98. ¹H NMR (400 Hz, DMSO) δ^1 8.044-7.174 (m, 12H), 5.430-5.423 (d, 2H), 4.159-4.075 (m, 2H); IR (KBr, cm^{-1}): 3433.61, 3024.42, 1633.00, 1587.53, 1412.10, 1090.25, 968.83, 829.65, 702.13.

Then, solid dipyph (2 mmol, 0.568 g) was dissolved in 50 mL DMF solvent. Fresh $\text{Cu}(\text{aceace})_2$ (4 mmol, 1.048 g) was added to this solution with stirring and the resulting solution was heated to refluxing. After 4.5 h, the reaction was stopped and the mix-



Scheme 1. Synthetic path for the bridged bidentate bipyridyl ligand of dipyph

ture was cooled to room temperature. The blue solution obtained was filtered and left to evaporate. A week later, the blue crystals of $[\text{Cu}_2(\text{C}_5\text{H}_7\text{O}_2)_4(\text{C}_{20}\text{H}_{16}\text{N}_2)]$ suitable for X-ray determination were obtained. Anal. Calcd (%): C, 59.46; H, 5.49; N, 3.47; Found (%): C, 59.33; H, 5.54; N, 3.66. IR (KBr, cm^{-1}): 3418.66, 3025.33, 1630.14, 1589.62, 1415.41, 973.72, 822.40, 556.56.

X-ray crystallography. The title complex was glued to a thin glass fiber with epoxy resin and collected on a Enraf-Nonius CAD-4 diffractometer with graphite-monochromated Mo K α radiation [$\lambda = 0.71073 \text{ \AA}$, $T = 293(2) \text{ K}$]. The crystallographic collection and refinement parameters for the compound are listed in Table 1. The empirical absorption correction was based on equivalent reflections, and other possible effects, such as absorption by the glass fiber, were simultaneously corrected. The structure of the complex was solved by direct methods and refined by least squares on F^2 . The hydrogen atom positions were fixed geometrically at calculated distances and allowed to ride on the parent carbon atoms and all non-hydrogen atoms were anisotropically refined. The SMART software was used for collecting frames of data, indexing reflections, and determination of lattice constants; SAINT-PLUS for integration of intensity of reflections and scaling; SADABS for absorption correction; and SHELXTL for space groups and structure determinations, refinements, graphics, and structure reporting.²³⁻²⁵

CCDC No. 786020 contains the supplementary crystallographic data for the title complex. These data can be obtained free of charge from The Cambridge Crystallographic Data Centre via www.ccdc.cam.ac.uk/data_request/cif.

Electrochemical measurement. The cyclic voltammetric (CV) measurements were performed on CHI 660 electrochemical workstation using a conventional three-electrode system, which consisted of a Pt working electrode and Pt auxiliary electrode,

an Ag/AgCl reference electrode (1 M KCl) and a scan rate of 200 mV/s. 0.1 M Tetrabutylammonium perchlorate (TBAP) was used as supporting electrolyte. The concentration of the title complex was $1.0 \times 10^{-3} \text{ M}$ in DMF solution. All the potential values are referenced to the Ag/AgCl electrode. Current-potential curve was displayed on an IBM computer using model 270 electrochemical analysis software.

Results and Discussion

Description of crystal structure. The perspective view of the title complex with atomic numbering scheme is shown in Figure 1 and Figure 2 shows the perspective view of the crystal packing in the unit cell. Some selected bond lengths and bond angles are listed in Table 2.

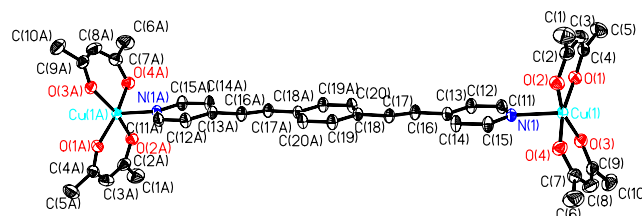


Figure 1. View of the title complex with 30% probability displacement ellipsoids (Hydrogen atoms are omitted for clarity).

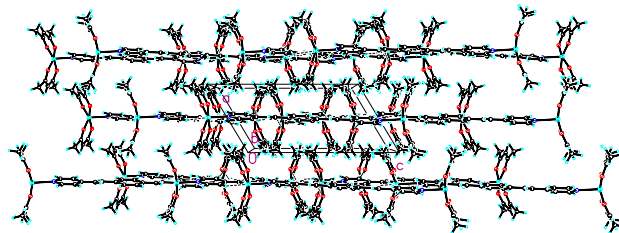


Figure 2. Packing diagram of the unit cell along the b -axis for the title complex.

Table 1. Crystallographic collection and refinement parameters for the title complex

| | |
|--|--|
| Empirical formula | $\text{C}_{40}\text{H}_{44}\text{Cu}_2\text{N}_2\text{O}_8$ |
| Formula weight | 807.85 |
| Crystal color | blue |
| Temperature | 273(2) K |
| Wavelength | 0.71073 \AA |
| Crystal system, Space group | Monoclinic, $P2_1/c$ |
| Unit cell dimensions | $a = 7.9584(16) \text{ \AA}$ $b = 18.594(4) \text{ \AA}$, $\beta = 120.97(2)^\circ$ $c = 15.063(4) \text{ \AA}$ |
| V , | 1911.2(8) \AA^3 |
| Z , Calculated density | 42, 1.404 Mg/m^3 |
| Absorption coefficient | 1.166 mm^{-1} |
| $F(000)$ | 840 |
| Theta range for data collection | 1.92 to 27.05° |
| Limiting indices | $-10 \leq h \leq 5$, $-23 \leq k \leq 21$, $-19 \leq l \leq 18$ |
| Reflections collected/unique | 8900/4017 [$R_{\text{int}} = 0.0241$] |
| Refinement method | Full-matrix least-squares on F^2 |
| Data/restraints/parameters | 4017/0/235 |
| Goodness-of-fit on F^2 | 1.099 |
| Final R indices [$I > 2\sigma(I)$] | $R_1 = 0.0537$, $wR_2 = 0.1285$ |
| R indices (all data) | $R_1 = 0.0672$, $wR_2 = 0.1357$ |
| Largest diff. peak and hole | -0.463 and $-0.226 \text{ e \AA}^{-3}$ |

Table 2. Selected bond lengths (\AA) and angles ($^\circ$) for the title complex

| Bond | Bond length (\AA) | Bond | Bond length (\AA) |
|-------------------|------------------------------|-------------------|------------------------------|
| Cu(1)-O(4) | 1.940(3) | Cu(1)-O(3) | 1.941(2) |
| Cu(1)-O(2) | 1.941(2) | Cu(1)-O(1) | 1.948(2) |
| Cu(1)-N(1) | 2.226(3) | O(1)-C(4) | 1.275(4) |
| O(2)-C(2) | 1.271(5) | O(4)-C(7) | 1.269(5) |
| O(3)-C(9) | 1.281(5) | N(1)-C(11) | 1.323(4) |
| C(11)-C(12) | 1.378(4) | C(4)-C(5) | 1.506(5) |
| C(1)-C(2) | 1.518(6) | C(16)-C(17) | 1.319(4) |
| C(18)-C(19) | 1.390(4) | C(18)-C(20) | 1.398(4) |
| Bond angle | Bond angle ($^\circ$) | Bond angle | Bond angle ($^\circ$) |
| O(2)-Cu(1)-O(1) | 91.54(11) | O(4)-Cu(1)-O(2) | 85.35(12) |
| O(4)-Cu(1)-O(3) | 92.29(12) | O(4)-Cu(1)-O(1) | 166.95(11) |
| O(4)-Cu(1)-N(1) | 96.58(11) | O(2)-Cu(1)-N(1) | 98.76(11) |
| O(3)-Cu(1)-N(1) | 98.02(10) | O(1)-Cu(1)-N(1) | 96.42(10) |
| O(2)-C(2)-C(3) | 124.8(4) | O(4)-C(7)-C(8) | 125.1(4) |
| C(11)-N(1)-C(15) | 115.7(3) | C(12)-C(13)-C(14) | 115.9(3) |
| C(17)-C(16)-C(13) | 126.8(3) | C(19)-C(18)-C(20) | 116.7(3) |

The structure unit of the title complex contains a pair of independent $[\text{Cu}_2(\text{aceace})_4(\text{dipyph})]$ molecules. Each of the molecule has an inversion center, which is located at the phenyl ring center. The coordination environments of the two Cu^{2+} ions are similar and each Cu^{2+} ion is pentacoordinated with four O atoms and one N atom in a distorted square pyramidal geometry, with the bond angles of O-Cu-O being in the range of $85.35(12)$ to $166.95(11)^\circ$ and O-Cu-N bond angles from $96.42(10)$ to $98.76(11)^\circ$. The basal coordination position are occupied by four O atoms from two acetylacetonate chelating ligands and the apical position is occupied by the N atom from a pyridyl ring of the bipyph, while the copper(II) atom is located in the center of the pyramid base with the Cu(II) atom apart from the pyramidal base being $0.251(1)$ Å. The Cu-O distances from $1.941(2)$ to $1.948(2)$ Å are all longer than those in the similar five-coordinated Cu complex of μ^2 -1,2-bis(2-pyridyl)ethene-bis((trifluoroacetylacetonato-O,O')-copper(II)) [Cu-O $1.926(2)$ - $1.937(4)$ Å]²⁶ and corresponding with those in (μ^2 -2,5-bis(2-pyridyl)ethynyl)thiophene)-tetrakis(1,1,1-trifluoroacetylacetonato)-di-copper(II) [Cu-O $1.935(3)$ - $1.956(4)$ Å].²⁷ The Cu-N distance of $2.226(3)$ Å is shorter than those in above two cited Cu complexes [Cu-N 2.315 Å²⁶ and 2.275 Å²⁷]. All of the bond lengths and bond angles in the phenyl rings and pyridyl rings are in the normal range. The pyridyl ring along with C(16) atom define a plane *P1* with the biggest deviation being -0.019 Å for C(12) atom and phenyl ring with the attached atoms of C(17) and C(17A) define another plane *P2* with the biggest deviation being 0.006 Å for C(18) and C(18A) atoms. The dihedral angle between above two planes is $1.50(2)^\circ$, and the biggest distance from the atoms in *P1* to the plane *P2* is $0.173(1)$ Å for atom C(14), which means that all of the atoms in the bidentate ligand of bipyph are almost coplanar.

In the crystal lattice, there exist some weak intermolecular interactions (see Table 3), including C-H \cdots π and C-H \cdots O interactions, which help to stabilize the molecular structure.

Magnetic property. The magnetic property of the title complex is depicted in Figure 3 with plot of molar magnetic susceptibility χ_m vs temperature *T*. As a whole, from temperature of 300 K changing to 2.0 K, the values of molar susceptibility χ_m do not change evidently. At first, χ_m changes slowly, and then it increases sharply from 0.00406 emu/mol at 30.0 K to 0.0644 emu/mol at 2.0 K. Magnetic susceptibility data between 2.0 K to 300.0 K obeyed the Curie-Weiss law $\chi_m = C/(T + \theta)$, with Curie constant $C = 0.1154$ emu·K/mol and Weiss constant $\theta =$

Table 3. Some weak intermolecular interactions^a

| D-H \cdots A | Symmetry code | D \cdots A (Å) | D-H \cdots A ($^\circ$) |
|----------------------------|-------------------|------------------|-----------------------------|
| C(14)-H(14A) \cdots O(2) | 1-x, -y, -z | 3.3706 | 172.62 |
| C(16)-H(16A) \cdots O(1) | x, 1/2-y, -1/2+z | 3.3318 | 146.69 |
| C(16)-H(16A) \cdots O(3) | x, 1/2-y, -1/2+z | 3.3131 | 136.02 |
| C(5)-H(5C) \cdots Cg(3) | 1+x, 1/2-y, 1/2+z | 3.6485 | 141.91 |
| C(1)-H(1B) \cdots Cg(4) | 1+x, y, 1+z | 3.6909 | 133.77 |
| C(1)-H(1B) \cdots Cg(4) | 2-x, -y, -z | 3.6909 | 133.77 |
| C(8)-H(8A) \cdots Cg(3) | -1+x, y, z | 4.0504 | 132.90 |

^aCg(3) and Cg(4) denote centroids of the pyridyl and phenyl rings, respectively.

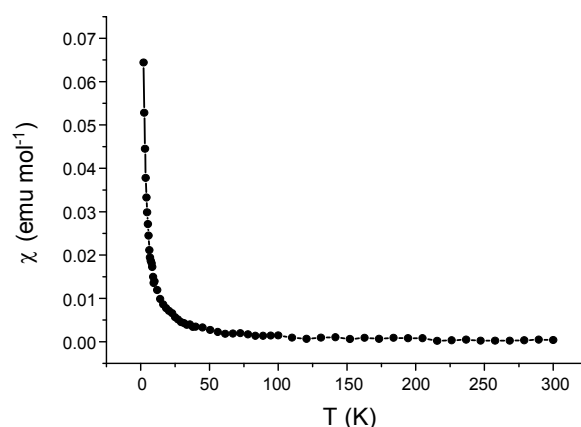


Figure 3. Temperature dependence of χ_m for the title complex.

-0.22 K, respectively. This behaviour suggests that a very weak antiferromagnetic interaction operate in the title complex.²⁸ The sample has effective magnetic moment μ_{eff} values of $0.9617\mu_B$ and $1.019\mu_B$ at 300.0 and 2.0 K, respectively, which is lower than the spin-only value for independent Cu^{2+} ion ($S = 1/2$, $\mu_{\text{eff}} = 1.73\mu_B$).

Thermal stability. The TG/DTG curves of the title complex are presented in Figure 4. As seen in Figure 4, the $[\text{Cu}_2(\text{aceace})_4(\text{dipyph})]$ undergoes two-step decomposition process and there are two endothermic peaks, one is at 228.1°C and another is at 306.9°C . The first step of weight loss (48.68%) occurs from 140°C to 240°C , which is approximately corresponding to the cleavage of two Cu-N bonds and two Cu-O bonds and the loss of one dipyph ligand and one acetylacetonate ligand (calcd. 47.40%). Then, from 260 to 800°C , the title complex takes place the second-time decompose and loses weight 26.10%, which is attributed to the breaking of another two Cu-O bonds and four C=O bonds and the loss of one acetylacetonate ligand and two $\text{CH}_3\text{CCHCH}_3$ groups of two acetylacetonate ligands except four O atoms (calcd. 28.83%). The final 25.22% residues are Cu_2O_4 (calcd. 23.76%).

Electrochemistry. The cyclic voltammetry behaviour of the title complex was studied and the results are shown in Figure 5. For the deoxygenated experiments, the electrolyte was bubbled

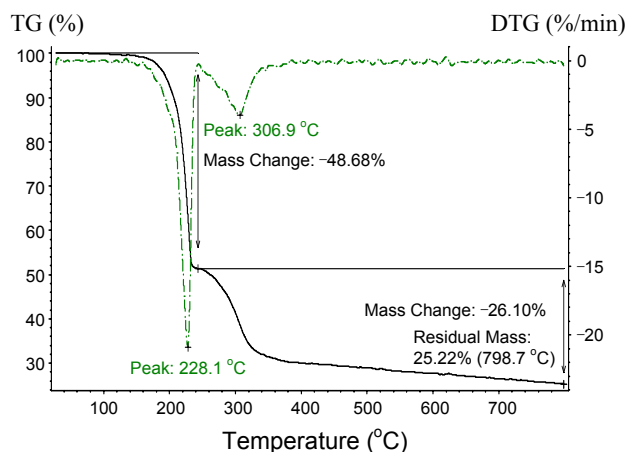


Figure 4. TG/DTG curves of the title complex.

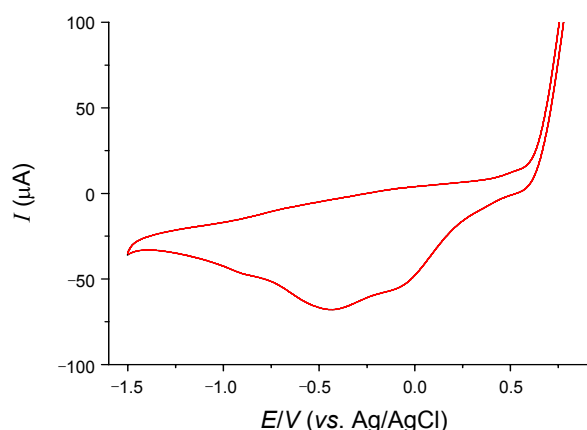


Figure 5. Cyclic voltammogram of the title complex in DMF ($0.1 \text{ mol}\cdot\text{L}^{-1}$ TBAP).

with purity nitrogen for 10 min and maintained nitrogen condition during the experiments. As seen from Figure 5, there are two cathodic peaks at -0.41 V and -0.05 V , respectively, while no oxidation is observed in the potential range of $-1.5 \text{ V} \sim 0.8 \text{ V}$, indicating that the electrochemical process of the title complex is irreversible.

Conclusion

Dinuclear Cu complex of $[\text{Cu}_2(\text{aceace})_4(\text{dipyph})]$ has been synthesized and its structure has been obtained by X-ray single crystal diffraction. The inversion center of the title complex is overlap with the center of the phenyl ring. Each of the Cu^{2+} ion adopts a square pyramid geometry and coordinates with four O atoms and one N atom. The magnetic property measurement shows that the title complex obeys the Curie-Weiss law and there exists a very weak antiferromagnetic interaction in the title complex. Thermal stability data reveal that the title complex carried out two-step decomposition process. Electrochemical determination presents an irreversible behaviour of the title complex.

Acknowledgments. This work was supported by Doctor Foundation of Shandong Province, P. R. China (No. BS2010CL021).

Supporting Information Available. Supporting Information are available on request from the correspondence author (fax: +86 532 84022948 email: zhaopusu@163.com).

References

1. Consiglio, G.; Failla, S.; Finocchiaro, P.; Oliveri, I. P.; Purrello,

- R.; Bella, S. D. *Inorg. Chem.* **2010**, *49*, 5134.
 2. Yin, P. X.; Zhang, J.; Li, Z. J.; Qin, Y. Y.; Cheng, J. K.; Zhang, L.; Lin, Q. P.; Yao, Y. G. *Cryst. Growth Des.* **2009**, *9*, 4884.
 3. Ghosh, A. K.; Jana, A. D.; Ghoshal, D.; Mostafa, G.; Ray Chaudhuri, N. *Cryst. Growth Des.* **2006**, *6*, 701.
 4. Kubo, Y.; Kitada, Y.; Wakabayashi, R.; Kishida, T.; Ayabe, M.; Kaneko, K.; Takeuchi, M.; Shinkai, S. *Angew. Chem. Int. Ed.* **2006**, *45*, 1548.
 5. Manna, S. C.; Zangrando, E.; Chaudhuri, N. R. *J. Mol. Struct.* **2008**, *877*, 145.
 6. Aakeröy, C. B.; Scott, B. M. T.; Smith, M. M.; Urbina, J. F.; Desper, J. *Inorg. Chem.* **2009**, *48*, 4052.
 7. Lipstman, S.; Goldberg, I. *Cryst. Growth Des.* **2010**, *10*, 1823.
 8. Felloni, M.; Blake, A. J.; Hubberstey, P.; Wilson, C.; Schröder, M. *Cryst. Growth Des.* **2009**, *9*, 4685.
 9. Seaton, C. C.; Parkin, A.; Wilson, C. C.; Blagden, N. *Cryst. Growth Des.* **2009**, *9*, 47.
 10. Zhang, J. P.; Lin, Y. Y.; Huang, X. C.; Chen, X. M. *Cryst. Growth Des.* **2006**, *6*, 519.
 11. Liang, X. Q.; Zhou, X. H.; Chen, C.; Xiao, H. P.; Li, Y. Z.; Zuo, J. L.; You, X. Z. *Cryst. Growth Des.* **2009**, *9*, 1041.
 12. Manna, S. C.; Ribas, J.; Zangrando, E.; Ray Chaudhuri, N. *Inorg. Chim. Acta* **2007**, *360*, 2589.
 13. Ma, M. L.; Li, X. Y.; Wen, K. *J. Am. Chem. Soc.* **2009**, *131*, 6733.
 14. Zhao, S. L.; Arachchige, S. M.; Slebodnick, C.; Brewer, K. J. *Inorg. Chem.* **2008**, *47*, 6144.
 15. Denning, M. S.; Irwin, M.; Goicoechea, J. M. *Inorg. Chem.* **2008**, *47*, 6118.
 16. Zeng, M. H.; Zou, H. H.; Hu, S.; Zhou, Y. L.; Du, M.; Sun, H. L. *Cryst. Growth Des.* **2009**, *9*, 4239.
 17. Cui, S. X.; Zhao, Y. L.; Zhang, J. P.; Liu, Q.; Zhang, Y. *Cryst. Growth Des.* **2008**, *8*, 3803.
 18. Bart, S. C.; Lobkovsky, E.; Bill, E.; Wiegardt, K.; Chirik, P. J. *Inorg. Chem.* **2007**, *46*, 7055.
 19. Fielden, J.; Sprott, J.; Long, D. L.; Kolgerler, P.; Cronin, L. *Inorg. Chem.* **2006**, *45*, 2886.
 20. McClard, R. W.; Holets, E. A.; MacKinnon, A. L.; Witte, J. F. *Biochem.* **2006**, *45*, 5330.
 21. Alessi, M.; Larkin, A. L.; Ogilvie, K. A.; Green, L. A.; Lai, S.; Lopez, S.; Snieckus, V. *J. Org. Chem.* **2007**, *72*, 1588.
 22. Sun, X. H.; Li, W.; Xia, P. F.; Luo, H. B.; Wei, Y.; Wong, M. S.; Cheng, Y. K.; Shuang, S. *J. Org. Chem.* **2007**, *72*, 2419.
 23. *SMART and SAINT for Windows NT Software Reference Manuals, Version 5.0*, Bruker Analytical X-Ray Systems, Madison, WI, 1997.
 24. Sheldrick, G. M. *SADABS- A Software for Empirical Absorption Correction*; University of Göttingen: Göttingen, Germany, 1997.
 25. *SHELXTL Reference Manual, Version 5.1*, Bruker Analytical X-Ray Systems, Madison, WI, 1997.
 26. Atienza, J.; Gutierrez, A.; Perpignan, M. F.; Sanchez, A. E. *Eur. J. Inorg. Chem.* **2008**, 5524.
 27. Delgado, S.; Medina, M. E.; Pastor, C. J.; Jimenez-Aparicio, R.; Priego, J. L. *Z. Anorg. Allg. Chem.* **2007**, *633*, 1860.
 28. Jian, F. F.; Xiao, H. L.; Wang, H. X.; Zhao, P. S.; Lu, L. D. *Chin. J. Inorg. Chem.* **2005**, *21*, 369.